Journal of Physics: Conference Series **338** (2012) 012020 doi:10.1088/1742-6596/338/1/012020

Kinetic approaches to phase transitions in strongly interacting matter

V Baran[1], M. Colonna[2], V. Greco[2,3], M. Di Toro[2,3], S. Plumari[2] and R. Zus[1]

[1] Physics Faculty, University of Bucharest, Romania
[2] Laboratori Nazionali del Sud INFN, I-95123, Catania, Italy
[3] Physics and Astronomy Dept., University of Catania, Italy

E-mail: baran@nipne.ro

Abstract. Strongly interacting matter manifests a very rich dynamical behavior and the associated phase diagram was intensively explored through heavy ions collisions during the last years. Around Fermi energies the nuclear multifragmentation shows up analogies with the liquid-gas phase transition. Within a microscopic transport model based on Boltzmann-Nordheim-Vlasov equation we investigate the kinetics of this process as well as the features related to the two-component character of the nuclear matter. The evolution of the fragmentation mechanism with the centrality and the role of various instabilities are also discussed. At ultra-relativistic energies recent results from RHIC and LHC experiments evidenced the manifestation of quarks and gluons degrees of freedom during the evolution of the hot fireball created in these collisions. Based on a relativistic transport model we inquire upon the role of chiral symmetry breaking on the collective features of expanding quark-gluon plasma.

1. Introduction

The fragment production in heavy ions reactions at intermediate energies represents an important dissipation mechanism. Very often, in discussing the nuclear multifragmentation, the analogy with the liquid-gas phase transition is invoked. However, in this comparison one should be aware of the differences determined by the Coulomb, finite-size or quantum effects. Moreover, at variance to the situation regarding the phase transitions in macroscopic systems, in heavy ions collisions the reaction times are comparable to the fragments growth time. The fast expansion may quench the system inside the instability region of the phase diagram and the spinodal decomposition will represent a significant kinetic mechanism for the fragment formation during the first stages of the nuclear fragmentation at Fermi energies. A binary system, including asymmetric nuclear matter (ANM), manifests a richer thermodynamical behavior since has to accommodate one more conservation law.

At ultra-relativistic energies, with the advance of new experimental programs ending with Relativistic Heavy Ion Collider (RHIC) at BNL and Large Hadron Collider (LHC) at CERN, the heavy ions collisions are probing new phases of strongly interacting matter. These investigations provide the means to test under extreme conditions of temperature and/or density the predictions of fundamental theory of strong interaction, Quantum Chromodynamics (QCD), by spanning different regions of the QCD phase diagram [1]. QCD is a non-Abelian gauge theory based on color SU(3) group and describes the interaction of quarks and gluons. It dictates the

structure of hadrons and nuclei and the interaction among them and has a very rich dynamical content. In particular it manifest the so called asymptotic freedom which means a decrease of the interaction strength with energy scale. At low energies, of the order of $\Lambda_{QCD} = 300MeV$, the coupling becomes large and a perturbation approach cannot be applied. Two important non-pertubative features of QCD are the color confinement, related to the fact that quarks and gluons are locally confined to color singlet bound states and spontaneous chiral symmetry breaking. This symmetry, which is exact in the limit of massless quarks, expresses the invariance of QCD Lagrangian density to global transformations $SU_L(N_F) \times SU_R(N_F)$, where N_F is the number of flavors, and is equivalent to invariance under $SU_V(N_F) \times SU_A(N_F)$. For one flavor case this leads to conservation of quark vector current $V^\mu(x) = \bar{q}(x)\gamma^\mu q(x)$ and of axial vector current $A^\mu(x) = \bar{q}(x)\gamma^\mu\gamma_5 q(x)$ respectively. Several experimental indications, including the masses of mesons and baryons of opposite parity and pion properties suggests that the chiral symmetry is realized in Nambu-Goldstone mode, i.e. the symmetry of the Lagrangian is not realized in the ground state. So the full chiral symmetry mentioned above is spontaneously broken down to the diagonal vector symmetry $SU_V(N_F)$. As a consequence it is expected the appearance in the spectrum of pseudoscalar mesons of mass zero, the Goldstone bosons. For two flavors case they are identified with the pions. Their mass small but finite, indicates an explicit breaking of the chiral symmetry as a consequence of non-zero bare (current) masses of up and down quarks (5 MeV and 10 MeV respectively). The pseudoscalar meson octet is associated to the Goldstone bosons in the three-flavor case but in this situation the explicit breaking symmetry is more evident since the mass of strange quark is greater, approx. 200 MeV.

In the first part of this work we discuss briefly the nature of the instabilities and of the related density fluctuations in binary systems. Then we describe some aspects of the kinetics of phase transition in ANM in the linear regime. For heavy ion collisions at intermediate energies, within a microscopic transport model, we explore the relevance of these results for nuclear multifragmentation and show the evolution of the fragmentation mechanisms with the centrality of the reaction.

At ultra-relativistic energies one of the important questions regards the the role of chiral symmetry breaking on quark-gluon plasma dynamics. Therefore in the second part of the paper, based on a relativistic transport model including a Nambu-Jona-Lasinio quark interaction, we investigate the influence of chiral symmetry breaking on the properties of the elliptic flow at RHIC energies.

2. Nuclear fragmentation at Fermi energies

The spinodal decomposition mechanism in the liquid-gas phase transition is related to the fact that dynamically the system can enter in the instability region of the phase diagram and is associated to the exponential amplification of density fluctuations.

An appropriate framework for the study of instabilities in two-components systems is provided by the Fermi liquid theory [2], which has been applied, for instance, to symmetric binary systems as SNM (the two components being protons and neutrons) [3] and the liquid ^3He (spin-up and spin-down components) [4, 5].

One-component systems may become unstable against density fluctuations as the result of the attractive interaction between constituents. In symmetric binary systems, like SNM, one may encounter two kinds of density fluctuations: isoscalar, when the densities of the two components fluctuate in phase with equal amplitude, and isovector when the two densities fluctuate still with equal amplitude but out of phase. Thermodynamically, the mechanical instability is associated to the instability against isoscalar fluctuations, leading to cluster formation, while chemical instability is related to instability against isovector fluctuations, leading to species separation.

An extension to asymmetric binary systems is obtained by a generalization of the formalism introduced in [4] to the asymmetric case. At $T = 0$ the thermodynamical stability requires the

energy of the system to be an absolute minimum for the undistorted distribution functions, so that the relation:

$$\delta H - \mu_p \delta\rho_p - \mu_n \delta\rho_n > 0 \tag{1}$$

is satisfied when we deform proton and neutron Fermi seas, determined by the distribution functions $f_q(\epsilon_p^q) = \Theta(\mu_q - \epsilon_p^q)$, $q = n, p$. Here H is the energy density, μ_q, ρ_q are the corresponding chemical potentials and densities.

The nucleons interaction is characterized by the Landau parameters:

$$F^{q_1 q_2} = N_{q_1} V^2 \frac{\delta^2 H}{\delta f_{q_1} \delta f_{q_2}} = N_{q_1} \frac{\delta^2 H}{\delta \rho_{q_1} \delta \rho_{q_2}} \tag{2}$$

$$N_q(T) = \int \frac{-2\ d\mathbf{p}}{(2\pi\hbar)^3} \frac{\partial f_q(T)}{\partial \epsilon_p^q} \tag{3}$$

where V is the volume and N_q is the single-particle level density at the Fermi energy. At $T = 0$ $N_q(0) = m p_{F,q}/(\pi^2\hbar^3) = 3\rho_q/(2\epsilon_{F,q})$, where $p_{F,q}$ and $\epsilon_{F,q}$ are Fermi momentum and Fermi energy of the q-component. Only monopolar deformations will be considered here and $F_{l=0}^{q_1 q_2}$ are the only non-zero Landau parameters. Eq.(1) becomes

$$\delta H - \mu_p \delta\rho_p - \mu_n \delta\rho_n = \frac{1}{2}(a {\delta\rho_p}^2 + b {\delta\rho_n}^2 + c \delta\rho_p \delta\rho_n) > 0 \tag{4}$$

where

$$\begin{aligned} &a = N_p(0)(1 + F_0^{pp}) \quad ; \quad b = N_n(0)(1 + F_0^{nn}) \quad ; \\ &c = N_p(0) F_0^{pn} + N_n(0) F_0^{np} = 2 N_p(0) F_0^{pn}. \end{aligned} \tag{5}$$

The r.h.s. of Eq.(4) is diagonalized by the following transformation:

$$\begin{aligned} u &= cos\beta\ \delta\rho_p + sin\beta\ \delta\rho_n, \\ v &= -sin\beta\ \delta\rho_p + cos\beta\ \delta\rho_n, \end{aligned} \tag{6}$$

where the *mixing* angle $0 \le \beta \le \pi/2$ is given by

$$tg\ 2\beta = \frac{c}{a-b} = \frac{N_p(0) F_0^{pn} + N_n(0) F_0^{np}}{N_p(0)(1 + F_0^{pp}) - N_n(0)(1 + F_0^{nn})}. \tag{7}$$

Then the condition (4) takes the form

$$\delta H - \mu_p \delta\rho_p - \mu_n \delta\rho_n = X u^2 + Y v^2 > 0 \quad , \tag{8}$$

where

$$\begin{aligned} X &= \frac{1}{2}(\ \ a + b + sign(c)\sqrt{(a-b)^2 + c^2}\ \ ) \\ &\equiv \frac{(N_p(0) + N_n(0))}{2}(\ 1 + F_{0g}^s\ ) \end{aligned} \tag{9}$$

and

$$\begin{aligned} Y &= \frac{1}{2}(\ \ a + b - sign(c)\sqrt{(a-b)^2 + c^2}\ \ ) \\ &\equiv \frac{(N_p(0) + N_n(0))}{2}(\ 1 + F_{0g}^a\ ), \end{aligned} \tag{10}$$

are defining the new generalized Landau parameters $F_{0g}^{s,a}$.

Hence, thanks to the rotation Eq.(6), it is possible to separate the total variation (see Eq.(1) into two independent contributions, the "normal" modes, characterized by the "mixing angle" β, which depends on the density of states and the details of the interaction. The thermodynamical stability requires $X > 0$ *and* $Y > 0$. Equivalently, the following conditions have to be fulfilled:

$$1 + F_{0g}^{s} > 0 \quad and \quad 1 + F_{0g}^{a} > 0, \tag{11}$$

representing the Pomeranchuk stability conditions extended to asymmetric binary systems. It can be proved that [6]:

$$\begin{aligned} XY &= N_p(0)N_n(0)[(1+F_0^{nn})(1+F_0^{pp}) - F_0^{np}F_0^{pn}] \\ &= \frac{[N_p(0)N_n(0)]^2}{(1-y)\rho^2}\left(\frac{\partial P}{\partial \rho}\right)_{T,y}\left(\frac{\partial \mu_p}{\partial y}\right)_{T,P} \end{aligned} \tag{12}$$

and:

$$\begin{aligned} \left(\frac{\partial P}{\partial \rho}\right)_{T,y} &= \frac{\rho y(1-y)}{N_p(0)N_n(0)}(\ t\ a + \frac{1}{t}\ b + c\ ) \\ \propto X(\sqrt{t}cos\beta + \frac{1}{\sqrt{t}}sin\beta)^2 &+ Y(\sqrt{t}sin\beta - \frac{1}{\sqrt{t}}cos\beta)^2 \\ with \quad t &= \frac{y}{1-y}\frac{N_n(0)}{N_p(0)}. \end{aligned} \tag{13}$$

Consequently the new stability conditions, Eq.(11), can be related to mechanical and chemical stability of the thermodynamical state, [7], i.e.

$$\left(\frac{\partial P}{\partial \rho}\right)_{T,y} > 0 \quad and \quad \left(\frac{\partial \mu_p}{\partial y}\right)_{T,P} > 0 \tag{14}$$

where P is the pressure and y the proton fraction. Indeed, let us assume that in the density range we are considering the quantities a and b remain positive. Then one can study the effect of the interaction between the two components, given by c, on the instabilities of the mixture. If $c < 0$, i.e. for an attractive interaction between the two components, the system is always stable against isovector-like fluctuations (see Eq.(10)) However it becomes unstable against isoscalar-like fluctuations if $c < -2\sqrt{ab}$ (see Eq.(9)). Thermodynamically this instability will show up as a chemical instability if $(-ta - b/t) < c < -2\sqrt{ab}$ or as a mechanical instability if $c < (-ta - b/t) < -2\sqrt{ab}$ (see Eq.(13)). We conclude that the relative strength of the interactions among the various species will determine the kind of thermodynamical instability which shows up. As we already mentioned, in the symmetric two-components systems it is a unique correspondence between the nature of thermodynamical instability and the nature of the unstable fluctuation. However we see that for asymmetric binary systems this correspondence is lost. The relevant instability region is defined only in terms of the instabilities against isoscalar fluctuations and therefore we can speak about a unique spinodal region. But inside the spinodal the system can be mechanically or chemically unstable. This is the case of asymmetric nuclear matter (ANM). For a Skyrme-like interaction, selected to reproduce the saturation properties of nuclear matter, $a, b > 0$ and $c < 0$, we deal only with isoscalar-like unstable fluctuations. We show in Fig.1, for three values of the proton fraction, the spinodal line corresponding to isoscalar-like instability (circles).

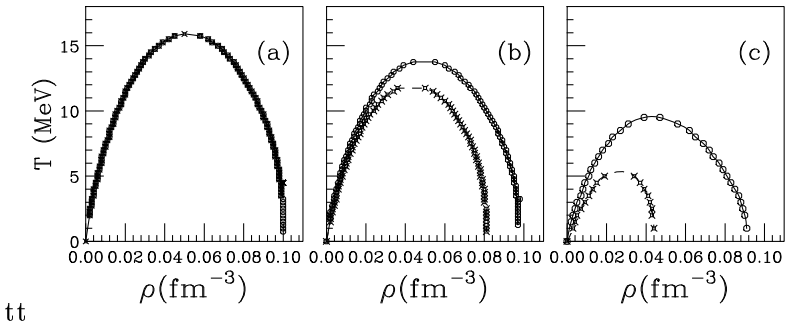

Figure 1. Spinodal boundary corresponding to insoscalar-like instability (circles) for three proton fractions: (a) $y = 0.5$, (b) $y = 0.25$, (c) $y = 0.1$. The mechanical instability line, inside spinodal region, is indicated by crosses.

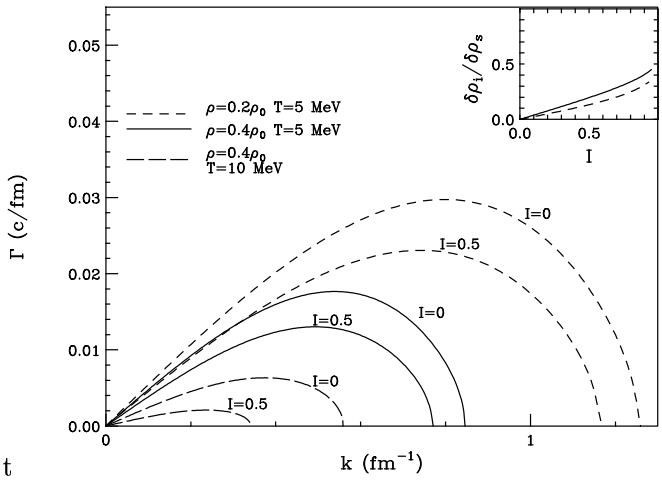

Figure 2. Growth rates of instabilities as a function of the wave vector, as calculated from the dispersion relation for three situations inside the spinodal region. Lines are labeled with the asymmetry value I. The insert shows the asymmetry of the perturbation $\delta\rho_I/\delta\rho_S$, as a function of the asymmetry I of the initially uniform system, for the most unstable mode, in the case $\rho = 0.4\rho_0$, $T = 5\ MeV$.

For asymmetric matter, $y < 0.5$, under this border one encounters either chemical instability, in the region between the two lines, or mechanical instability, under the inner line (crosses). The latter is defined by the set of values (ρ, T) for which $\left(\frac{\partial P}{\partial \rho}\right)_{T,y} = 0$.

To complete our analysis we consider now the case $c > 0$, i.e. when the interaction between the two components is repulsive. Now the thermodynamical state is always stable against isoscalar-like fluctuation. In can becpme unstable to isovector fluctuations if $c > 2\sqrt{ab}$. With our choices of the parameters, $a, b, c > 0$, the isovector instability is always associated with chemical instability. Such situation will lead to a component separation of the liquid mixture while the total density does not change. Summarizing, a complete analysis of the instabilities of any binary system can be performed, in connection to signs, strengths and density dependence of the interactions among the components.

Once the stability conditions of ANM were investigated, the linear response will provide informations about the growing rate of the unstable modes, relevant for the fragment formation

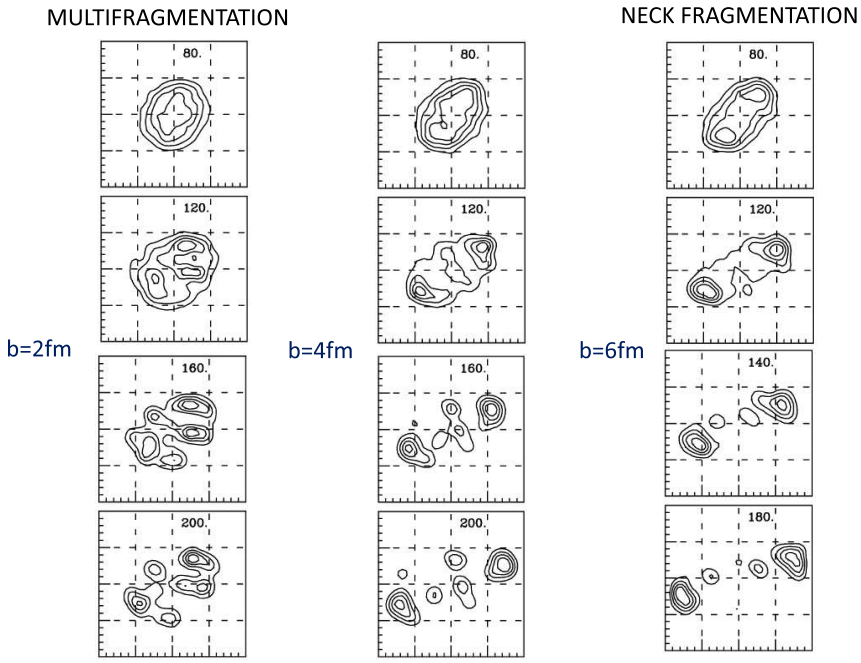

Figure 3. Density contour plots for $^{124}Sn + ^{124}Sn$ collision at 50AMeV for three impact parameters. From the left b=2 fm, b=4 fm and b=6fm.

time scales in multifragmentation. The approach is based on Vlasov equation,

$$\frac{\partial f_q(\mathbf{r},\mathbf{p},t)}{\partial t} + \frac{\mathbf{p}}{m}\frac{\partial f_q}{\partial \mathbf{r}} - \frac{\partial U_q(\mathbf{r},t)}{\partial \mathbf{r}}\frac{\partial f_q}{\partial \mathbf{p}} = 0 \ , \qquad q = n, p. \tag{15}$$

where $U_q(\mathbf{r},t)$ is the self-consistent mean field potential in a Skyrme-like form [8, 9]. By linearization, corresponding to a semiclassical RPA approach, it is obtained a dispersion relation quadratic in the frequency ω of the mode $\delta f_q(\mathbf{r},\mathbf{p},t) \sim \exp(-i\omega t)$. One finds two independent solutions (isoscalar-like and isovector-like solutions): ω_s^2 and ω_i^2. For the unstable isoscalar-like mode we report in Fig.2 the growth rate Γ = Im $\omega(k)$ as a function of the wave vector k. Results are shown for symmetric ($I = 0$) and asymmetric ($I = 0.5$) nuclear matter.

The growth rate has a maximum $\Gamma_0 = 0.01 \div 0.03$ c/fm corresponding to a wave-vector value around $k_0 = 0.5 \div 1$ fm^{-1} and becomes equal to zero at $k \simeq 1.5k_0$, due to k-dependence of the Landau parameters. The instabilities are reduced when increasing the temperature, an effect also present in the symmetric N = Z case [10, 11, 12]. At larger initial charge asymmetry the development of the spinodal instabilities is slower. The conclusion is that the fast spinodal decomposition mechanism in neutron-rich matter will dynamically leads to more symmetric fragments surrounded by a more netron rich gas. Some recent experimental observations from fragmentation reactions with neutron rich nuclei at the Fermi energies seem to be in agreement with this result: nearly charge symmetric Intermediate Mass Fragments (IMF) have been detected together with very neutron-rich light ions [13]. All these considerations provide a firm ground for numerical simulations performed in the nonlinear regime, corresponding to realistic initial conditions of heavy-ions collisions at Fermi energies. In Fig. 3 we show the evolution of the reaction mechanism with the impact parameter. A transition from multifragmentation, at $b = 2fm$, to neck fragmentation, at $b = 6fm$, is observed. These results were obtained within a microscopic transport model, Stochastic Mean Field (SMF)[14]. Fragment formation and growth is quite consistent with spinodal decomposition mechanism. The velocity distributions of the fragments are in agreement with several experimental observations. Based on these approaches the correlations between fragments isopin content, velocity distributions and IMF flows open the

possibility to learn more about the density dependence of the symmetry energy in the equation of state, of interest in the study of exotic nuclei or astrophysical investigations [14].

3. Transport approach to QGP expansion including chiral symmetry breaking

The difficulties encountered in the basic theory in the nonperturbative regime motivates to look at simpler models which are capturing some essential features of QCD. One of the models appropriate to study the chiral symmetry breaking is the Nambu-Jona-Lasinio (NJL) model. The NJL Lagrangian density contains only quark degrees of freedom and the effects of gluons are included in a four fermion point interaction. Hence we deal with an effective field theory with an attractive force between quarks and antiquarks whose Lagrangian density (for one-flavor case) is

$$\mathcal{L}_{NJL} = \bar{q} i\gamma^{\mu}\partial_{\mu} q + G[(\bar{q}q)^2 + (\bar{q} i\gamma_5 q)^2] \tag{16}$$

where $(\bar{q}q)^2 \equiv \left(\sum_{a=1}^{N_c} \bar{q}^a q^a\right)^2$ and N_c is the number of color degrees of freedom. The coupling constant G is assumed to be positive so that the forces between quarks and antiquarks are attractive. In analogy with the superconductivity, where an attractive interaction between electrons with opposite momenta at Fermi surface leads to a non-pertubative change of ground state, the quark-antiquark interaction generate a similar ground state built as a coherent superposition of quark-antiquark pairs with zero total momentum and zero total helicity. A BCS approach is then possible with a variational ground state [15]:

$$|vac\rangle = \prod_{\mathbf{p},s=\pm 1} [\, \cos\theta(p) - s \sin\theta(p) b^{\dagger}(\mathbf{p},s) d^{\dagger}(-\mathbf{p},s)]|0\rangle \tag{17}$$

The annihilation operators for quarks and antiquarks with momentum p and helicity s define the normal (perturbative) vacuum, i.e. $b(\mathbf{p},s)|0\rangle = d(\mathbf{p},s)|0\rangle = 0$. The variational principle leads to an equation analogous to the gap equation in superconductivity:

$$m^* = 4GN_cN_f \int_0^{\Lambda} \frac{d^3q}{(2\pi)^3} \frac{m^*}{E_q} \tag{18}$$

where $E_q = \sqrt{q^2 + m^{*2}}$ and $\sin\theta(p) = m^*/\sqrt{p^2 + m^{*2}}$. The three momentum cut-off parameter Λ was introduced since the point-like interaction in the NJL Lagrangian renders the model nonrenormalizable. For $N_F = 2$ the model contains three free parameters: the coupling constant G, the current quark mass m and the cutoff Λ which is used to make theory finite. These are fixed to reproduce the physical pion mass, $m_\pi = 135MeV$, the physical pion decay constant $f_\pi = 93MeV$ and the chiral condensate value $\langle\bar{\psi}\psi\rangle = \dfrac{m^* - m}{2G}$. The latter, which is the order parameter of the phase transition, having zero value in the chiral restored phase, has larger uncertainties and therefore different sets of parameters are possible. For example in [16] with the set $\Lambda = 820MeV, G\Lambda^2 = 1.99, m = 4.0MeV$ is obtained $m^* = 323MeV$ while in [17] with $\Lambda = 588MeV, G\Lambda^2 = 2.44, m = 5.6MeV$ is obtained $m^* = 400MeV$.

The NJL model can be extended to finite density and temperature [18]. The mass gap equation, including a current finite current mass becomes:

$$M(T,\mu) = m + 4\,G\,N_c M(T,\mu) \int \frac{d^3p}{(2\pi)^3} \frac{1 - f^-(T,\mu) - f^+(T,\mu)}{E_p} \tag{19}$$

with $E_p = \sqrt{p^2 + M(T,\mu)^2}$ and $f^-(T,\mu)$ $f^+(T,\mu)$ the Fermi-Dirac distribution functions for quarks and antiquarks respectively. The solution of this equation for various temperatures as a

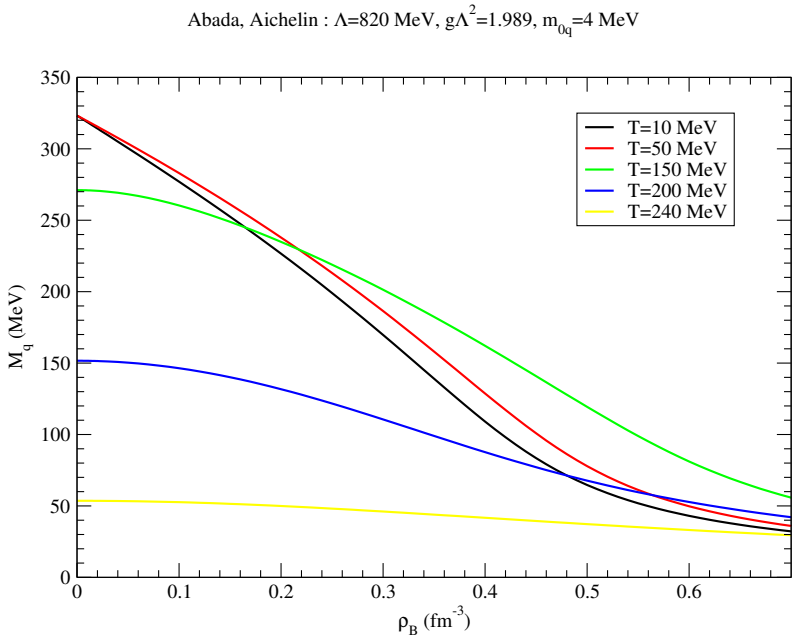

Figure 4. Quark constituent mass as a function of barionic density for various temperatures

function of barionic density with the set of parameters from [16] is plotted in Fig. 5. Thermal fluctuations as well as larger barionic densities are reducing the effect of symmetry breaking.

The theoretical views on QGP changed dramatically with the discoveries at RHIC from a system of gas of dressed quarks and gluons interacting weakly with each other to a strongly interacting matter of tightly coupled qusiparticles, an "perfect fluid (that) quenches jets almost perfectly" [19]. Within a standard scenario the evolution of the system following the heavy ions collision begin with the generation of an intense chromofields which later decay into of quarks and gluons. Then take place thermalization and entropy production, a viscous hydrodynamical expansion and hadronization. Important signals for QGP formation at RHIC includes strong azimuthal dependence of particle momenta described by the elliptic flow. Moreover the valence quark scaling of elliptic flow parameter v_2 indicates that flow pattern is developed at quark level.

One of the interesting questions is to understand the role of chiral symmetry breaking on collective features of expanding QGP. We solved numerically the microscopic transport equations of NJL model employing the test particle method [28]. One finally obtains the Boltzmann-Vlasov transport equations for the (anti-) quark phase-space distribution function $f^{\pm}$:

$$p^{\mu}\partial_{\mu}f^{\pm}(x,p) + M(x)\partial_{\mu}M(x)\partial_{p}^{\mu}f^{\pm}(x,p) = \mathcal{C}(x,p) \tag{20}$$

where $\mathcal{C}(x,p)$ is the Boltzmann-like collision integral, main ingredient of the several cascade codes already developed [20, 21, 22]. We notice that in addition to the cascade model ingredients the NJL dynamics introduces a new term associated to the mass generation. The Eq.(20) is formally the same as the widely used relativistic transport approaches for hadronic matter like RBUU,uRQMD, RLV [23, 24], but with a vanishing vector field. A key difference is however that particles do not have a fixed mass and a self-consistent approach couples the transport Eq.(20) to the mass gap equation of the NJL model that extended to the case of non-equilibrium as:

$$\frac{M(x)-m}{4\,G\,N_c} = M(x)\int\frac{d^3p}{(2\pi)^3}\frac{1-f^{-}(x,p)-f^{+}(x,p)}{E_p(x)} \tag{21}$$

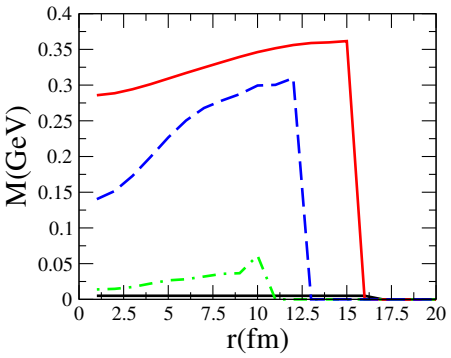

Figure 5. Quark constituent mass as a function of radial distance from the center of the expanding distribution Green dot dashed line: t=0.67 fm/c.Blue dashed line:t=3.7 fm/c. Red solid line:t=6.7 fm/c.Black line: current quark mass.

This equation determines the local mass $M(x)$ at the space-time point x in terms of the distribution functions $f^{\pm}(x,p)$. The Eqs.(20) and (21) form a closed system of equations constituting the Boltzmann-Vlasov equation associated to the NJL Lagrangian that allows to obtain self-consistently the local effective mass $M(x)$ and time dependent, nonequilibrium distribution function $f^{\pm}(x,p)$.

We have run the simulations for $Au+Au$ at $\sqrt{s_{NN}}=200$ AGeV and $b=6\,fm$. The density distribution in coordinate space is given by the standard Glauber model. The maximum initial temperature is $T=340$ MeV and the initial time is $\tau_0=0.6$ fm/c as usually done also in hydrodynamical calculations. We follow the dynamical evolution of quarks, anti-quarks and gluons. The last has been included, even if they are not explicitly present in the NJL model, with the aim of using a realistic density for both the total and the (anti-)quark density in the simulation of the collisions. However gluons do not actively participate in the evaluation of the chiral phase transition, but they simply acquire the same mass of the quarks not contributing to its determination according to the the NJL model. The justification for this choice relies on the quasi-particle models that are fitted to lQCD thermodynamics [25, 26] where one finds a similar behavior of $M(T)$ for both gluons and quarks approximately.

In Fig. 5 plot the radial dependence of the quark constituent mass at three different instants: initial time $t=0.6fm/c$, $t=3.6fm/c$ and final time $t=6.7fm/c$. The mass is larger toward the frontiers of the expanding distributions where the quark densities are lower. For comparison, in the case without NJL interaction, the mass is constant, equal to the current mass.

In Fig. 6 (right) it is shown the time evolution of the average elliptic flow $\langle v_2\rangle$ for a constant transport cross section of σ_{tr} =10 mb, a typical value that is able to reproduce the amount of v_2 observed in experiments [27]. Comparing the two lines we can see that the NJL mean field induce a decrease of $\langle v_2\rangle$. The reduction of v_2 can be expected considering that the NJL field produce a scalar attractive field that at the phase transition results in a gas of massive particles.

In Fig.6 (left), we show the elliptic flow at freeze-out as a function of the transverse momentum p_T. One can see that the role of the mean field even increases with momentum affecting also particles at a p_T larger than the energy scale of the scalar condensate $\langle\bar{\psi}\psi\rangle\sim 300MeV$. Therefore the effect of the scalar field extends thanks to collisions into a range quite larger than one would naively think and the interplay between collisions and mean field is fundamental. We also find that at $b=7fm$ the presence of a NJL-field that drives the chiral phase transition suppress the $v_2(p_T)$ by about 20% at $p_T>1$ GeV [28], [29].

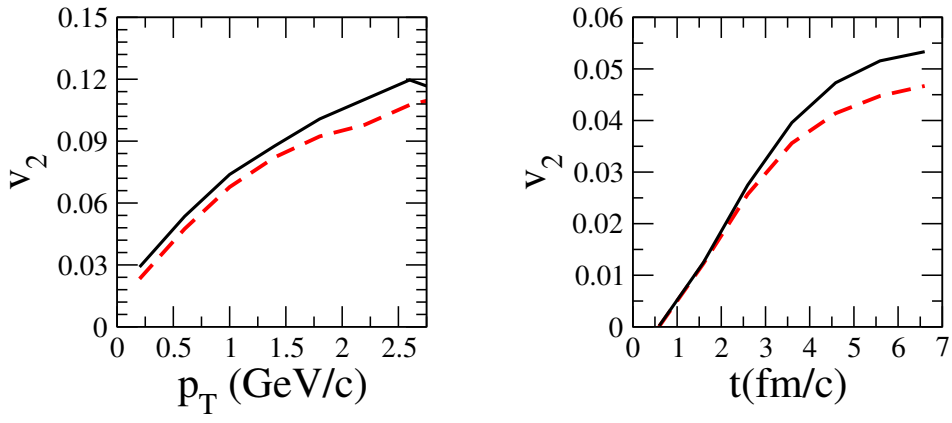

Figure 6. Left: Average elliptic flow as a function of transverse momentum for $Au + Au$ collisions in the mid-rapidity region $|y| < 1$ at b= 6 fm. Right: time evolution of the elliptic flow parameter for the same case as in the left panel. Black solid: only collisions. Red dashed:NJL mean field included.

4. Conclusions and perspectives

In this work we explored several facets of the nuclear fragmentation at Fermi energies. This can be related to a spinodal decomposition mechanism and realistic simulations based on microscopic transport models provide important informations related to the nuclear EOS. We then investigated within a relativistic transport model the effects of chiral symmetry breaking on the collective features of quark-gluon plasma at RHIC conditions. A sizable lowering of elliptic flow parameter was observed. The approach can be extended to LHC conditions and is appropriate to study the effects of fixed shear viscosity to entropy density ratio in the presence or absence of chiral dynamics. By including other interaction terms the transport model can be applied to situations corresponding to a finite barionic density.

Acknowledgments

This work for V. Baran was supported by a grant of the Romanian National Authority for Scientific Research, CNCS-UEFISCDI, project number PN-II-ID-PCE-2011-3-0972. S. Plumari and V. Greco are partially supported by the FIRB Research Grant RBFR0814TT. For R. Zus this work was supported by the strategic grant POSDRU/89/1.5/S/58852, Project "Postdoctoral programme for training scientific researchers" co-financed by the European Social Found within the Sectorial Operational Program Human resources Development 2007-2013.

References

[1] *Quark-Gluon Plasma* 2010, ed. Rudolph C Hwa and Xin-Nian Wang, Vol 4, (World Scientific)
[2] Landau L D 1957 JETP **5** 101
[3] Migdal A B 1967 *Theory of finite Fermi systems and applications to atomic nuclei*, (Wiley & Sons, N.Y.)
[4] Baym G and Pethick C J 1978 *The physics of Liquid and Solid Helium* vol 2, ed. K.H.Bennemann and J.B.Ketterson, Vol 2, (Wiley, N.Y.), p 1
[5] Pethick C J and Ravenhall D G 1988 *Ann.Phys.* **183** 131
[6] Baran V, Colonna M, Di Toro M and Greco V 2001 *Phys. Rev. Lett.* **86** 4492
[7] Landau L D and Lifshitz E M 1989 *Statistical Physics*, (Pergamonn Press), p. 288
[8] Colonna M, Di Toro M and Larionov A B 1998 *Phys.Lett.* B**428** 1
[9] Baran V, Colonna M, Di Toro M and Larionov A B 1998 *Nucl.Phys.* A **632** 287
[10] Colonna M and Chomaz P H 1994 *Phys.Rev.* C **49** 1908
[11] Colonna M, Chomaz P H and Randrup J 1994 *Nucl.Phys.* A**567** 637
[12] Chomaz P H, Colonna M and Randrup J 2004 *Phys.Rep.* **389** 263

[13] Xu H S et al. 2000 *Phys.Rev.Lett.* **85** 716
[14] Baran V, Colonna M, Di Toro M and Greco V 2005 *Phys. Rep.* **410** 335
[15] Klevansky C D 1992 *Rev. Mod. Phys.* **64** 649
[16] Abada A and Aichelin J 1995 *Phys. Rev. Lett.***74** 3130
[17] Buballa M 2005 *Phys. Rep.***407** 205
[18] Klevansky C D 1996 *Ann. Phys.***245** 445
[19] Muller B 2009 *Prog. Part. Nucl. Phys.***62** 551
[20] Molnar D and Gyulassy M 2002 *Nucl.Phys* A **697** 495
[21] Xu Z and Greiner C 2005 *Phys. Rev.* C **71** 064901
[22] Ferini G, Colonna M, Di Toro M and Greco V 2009 *Phys Lett* B **670** 325
[23] Bass S A et al. 1998 *Prog.Part. Nucl. Phys.***41** 255
[24] Fuchs C and Wolter H H 1995 *Nucl. Phys.* A**589** 732
[25] Levai P and Heinz U W 1998 *Phys. Rev* C **57** 1879
[26] Plumari S, Alberico W M, Greco V and Ratti C *preprint arXiV.hep-ph/:1103.5611*
[27] Lin Z-W and Ko C M 2002 *Phys. Rev.* C **65** 034904
[28] Plumari S, Baran V, Di Toro M, Ferini G and Greco V 2010 *Phys.Lett.* B **689** 18
[29] Plumari S 2010 *PhD thesis* (Univ. of Catania,Italy)